

# A Novel Long Non-Coding RNA (*Ctcflos*) Modulates Glucocorticoid Receptor-Mediated Induction of Hepatic Phosphoenolpyruvate Carboxykinase in Mice

Jae-Yeon Yoon (✉ [yjaeyeun@snu.ac.kr](mailto:yjaeyeun@snu.ac.kr))

Seoul National University College of Pharmacy

Ju-Yeon Kim

Seoul National University College of Pharmacy

Na-Lee Ka

Seoul National University College of Pharmacy

Sang-Heon Lee

Seoul National University College of Pharmacy

Mi-Ock Lee

Seoul National University <https://orcid.org/0000-0002-1578-8211>

---

## Research

**Keywords:** CTCFLOS, PEPCK, GR, lncRNA, hnRNPL

**Posted Date:** October 26th, 2021

**DOI:** <https://doi.org/10.21203/rs.3.rs-1002551/v1>

**License:**   This work is licensed under a Creative Commons Attribution 4.0 International License.

[Read Full License](#)

---

# Abstract

## Background

Phosphoenolpyruvate carboxykinase (*Pck1*) is a key enzyme that catalyzes an irreversible step of hepatic gluconeogenesis; however, the mechanism underlying *Pck1* regulation is not fully understood. This study aims to identify a lncRNA that regulates transcription of the *Pck1* gene.

## Methods

The precise structures of five different hepatic *Ctcflos* isoforms were identified through rapid amplification of cDNA ends in the mouse liver. The expression level of hepatic *Ctcflos* level was determined by PCR and the role of *Ctcflos* were assessed using antisense oligonucleotides and virus encoding *Ctcflos* both *in vitro* and *in vivo*. The target protein interacted with *Ctcflos* was identified through RNA pull down assay. Contribution of *Ctcflos* in glucocorticoid receptor (GR)-mediated *Pck1* gene expression was evaluated by chromatin immunoprecipitation, co-immunoprecipitation, *in situ* proximity ligation assay, and reporter gene analysis.

## Results

A novel lncRNA *Ctcflos* was identified in the enhancer region of *Pck1* gene. Induction of *Ctcflos* was dependent on the glucocorticoid receptor (GR) in the livers of fasted or dexamethasone-administered mice. Overexpression of *Ctcflos* by infusion of an adenovirus encoding *Ctcflos* increased transcript- and protein-level of *Pck1*, whereas knockdown of *Ctcflos* using antisense oligonucleotides suppressed. RNA pulldown experiments showed that *Ctcflos* bound the heterogeneous ribonucleoprotein L (hnRNPL) which interacts with GR. Interestingly, knockdown of hnRNPL upregulated the *Pck1* gene. Finally, we found that, in the presence of *Ctcflos*, the binding between GR and hnRNPL was weakened, whereas the DNA binding of GR was enriched in the *Pck1* enhancer region.

## Conclusions

We report the discovery of a novel lncRNA, *Ctcflos*, that regulates the transcription of *Pck1* by modulating GR function. Targeting *Ctcflos* may provide a new insight into the development of alternative treatments for hyperglycemia by offering specific regulation of hepatic *Pck1* gene expression.

## Introduction

Glucose homeostasis is tightly regulated to meet energy demands during the feeding and fasting cycle in mammals. The liver is a central organ in the regulation of glucose metabolism in response to the feeding and fasting transitions (Rui, 2014). In the fasted condition, the pancreatic hormone glucagon and the

adrenal hormone glucocorticoid are secreted to enhance hepatic glucose production and maintain the level of glucose in the blood within a narrow range (Rui, 2014; Saltiel and Kahn, 2001). Glucagon triggers gluconeogenesis in the liver via the cAMP/protein kinase A signaling pathway, which induces the expression of the peroxisome proliferator-activated receptor  $\gamma$  coactivator 1 $\alpha$  (PGC1 $\alpha$ ). In turn, PGC1 $\alpha$  coactivates transcription factors, including the glucocorticoid receptor (GR, NR3C1), hepatocyte nuclear factor 4 $\alpha$ , and forkhead box O1, to activate hepatic gluconeogenesis (Puigserver et al., 2003; Yoon et al., 2001). The rate of gluconeogenesis is determined by the expression and activation of a key gluconeogenic enzyme, i.e., cytoplasmic phosphoenolpyruvate carboxylase (Pck1), which converts cytoplasmic oxaloacetate to phosphoenolpyruvate irreversibly (Jitrapakdee, 2012). The hyperglycemia resulting from the abnormal elevation of hepatic glucose production causes organ damage because of increased oxidative stress and apoptosis (Volpe et al., 2018). Thus, the factors that modulate the expression level of Pck1 are of great importance in controlling hyperglycemia.

The expression of Pck1 is multi-hormonally controlled at the transcription level, which is unlikely for most metabolic enzymes, which are the subject of allosteric or other posttranslational regulation. In fact, many hormone-responsive elements that are sensitive to insulin, i.e., GR, cAMP, and thyroid hormone, are found in the promoter of the *Pck1* gene (Hanson and Reshef, 1997; Yang et al., 2009). Among the hormone-dependent transcription factors, GR has long been known to stimulate the transcription of the *Pck1* gene (Imai et al., 1990). Once glucocorticoid binds to GR, the glucocorticoid-GR complex is translocated to the nucleus, where it binds to glucocorticoid responsive elements (GREs), generally AGAACAnnnTGTTCT, in its target promoters (Weikum et al., 2017). The GREs in the *Pck1* promoter are complicated in that GR cooperates with diverse accessory factors at multiple GREs surrounded by or overlapping with other response elements (Chakravarty et al., 2005). Recently, it was reported that the GR-binding sites are highly distributed in the intergenic or intronic region, which could be the enhancer rather than the promoter (Grontved et al., 2013). In recent years, it has been well established that not only promoters, but also enhancer regions, are associated with gene transcription through epigenetic histone modifications (Gates et al., 2017). In particular, transcriptionally active enhancers are marked by abundant methylation of histone H3 at lysine 4 (H3K4me1) and acetylation of histone H3 at lysine 27 (H3K27ac), whereas the promoters of genetically active sites are enriched with trimethylation of histone H3 at lysine 4 (H3K4me3), acetylation of histone H3 at lysine 9 (H3K9ac), and H3K27ac (Gates et al., 2017). Increased marks of H3K4me1 in the enhancer play active regulatory roles as chromatin remodelers by recruiting the chromatin-remodeling complex to the enhancer region (Local et al., 2018). The enhancer may encode an enhancer RNA (eRNA) that regulates the expression of neighboring target genes by modulating the promoter-enhancer interaction or chromatin remodeling (Sartorelli and Lauberth, 2020). Recently, the involvement of GR in the regulation of eRNAs has been demonstrated, particularly in the inflammatory responses of pulmonary epithelial cells and hepatic lipid metabolism in mice (Mostafa et al., 2021; Roqueta-Rivera et al., 2016; Sasse et al., 2019). However, such enhancer regions regulated by GR have not been revealed in the transcription of the *Pck1* gene.

Long non-coding RNAs (lncRNAs) are a class of RNA defined as transcripts that are at least 200-nucleotides (nt) long with an exon-intron structure but no coding potential (Statello et al., 2021).

Recently, important roles in numerous physiological functions have been reported for many nuclear and cytoplasmic lncRNAs (Statello et al., 2021). Nuclear lncRNAs regulate the transcription of neighboring (acting in *cis*) or distant (acting in *trans*) genes by recruiting or sequestering transcription factors or epigenetic modifiers in the regulatory region of the neighboring genes (Kopp and Mendell, 2018). Some nuclear lncRNAs affect the alternative splicing, compartmentalization, and nuclear export of nuclear mRNAs (Statello et al., 2021). Recently, a class of lncRNA generated from an enhancer region and acting as an eRNA, but with most of the features of lncRNAs, was reported and termed enhancer-associated lncRNA (elncRNA) (Li et al., 2016). In the past decade, many lncRNAs that regulate glucose metabolism have been identified in the human and mouse liver (Zhao et al., 2017). For example, lncLGR suppresses hepatic glucokinase expression and glycogen storage by interacting with hnRNPL during fasting in mice (Ruan et al., 2016). Moreover, lncSHGL suppresses hepatic gluconeogenesis and lipogenesis by recruiting hnRNPA1 (Wang et al., 2018). The lncRNA Gm10804 enhances the levels of gluconeogenic enzymes, including *Pck1* and *G6Pase*, in hepatocytes, and knockdown of Gm10804 *in vivo* ameliorates disorders of hepatic glucose and lipid metabolism in diabetes with non-alcoholic fatty liver disease (Li et al., 2020). However, an lncRNA that directly controls the transcriptional expression of the *Pck1* gene has not been identified.

Here, we report the discovery of a liver-enriched lncRNA, *Ctcflos*, which is encoded in the enhancer region of the mouse *Pck1* gene. The expression of *Ctcflos* was induced under fasting status and enhanced the expression of *Pck1* at the transcription level in a GR-dependent manner through binding to hnRNPL, which represents a novel regulatory mechanism of regulation of *Pck1* gene transcription.

## Materials And Methods

### Cell Culture and Subcellular Fractionation

Primary mouse hepatocytes were isolated from 8–10-week-old male C57BL/6N mice as described previously (Kim et al., 2012). The liver was perfused with Hanks' Balanced Salt Solution containing 0.05 mM ethylene glycol tetra acetic acid for 3 min, followed by a solution containing 0.05% collagenase type IV (Merck, Darmstadt, Germany). After centrifugation at 500 rpm for 3 min, the cell pellet containing hepatocytes was plated in collagen-coated plates with Medium 199 (HyClone, Logan, UT) supplemented with 10% fetal bovine serum, 23 mM HEPES, and 10 nM dexamethasone and maintained under 5% CO<sub>2</sub> and 95% air at 37°C. AML12 cells were obtained from the American Type Culture Collection and cultured in DMEM/F-12 medium supplemented with insulin–transferrin–selenium (ITS-G; Thermo Fisher Scientific, Waltham, MA), dexamethasone (Sigma-Aldrich, St Louis, MO), and antibiotics under 5% CO<sub>2</sub> and 95% air at 37°C. Subcellular fractionation was performed as described previously (Miao et al.). Briefly, primary hepatocytes were resuspended in a buffer containing 10 mM HEPES, pH 7.9, 1.5 mM MgCl<sub>2</sub>, 10 mM KCl, 0.5 mM DTT, and a protease inhibitor and incubated on ice for 15 min. After adding 0.5% NP-40, the mixture was vortexed vigorously and centrifuged. The supernatant was saved as the cytoplasmic fraction. The precipitated nuclear pellet was resuspended in a 50% glycerol buffer and mixed with nucleus lysis buffer (20 mM HEPES pH 7.9, 7.5 mM MgCl<sub>2</sub>, 0.2 mM EDTA, 0.3 M NaCl, 1 M urea, 1% NP-

40, and 1 mM DTT) and centrifuged. The supernatant was collected as the nucleoplasmic fraction. The remaining chromatin pellet was washed with cold phosphate-buffered saline and saved as the chromatin fraction. Easy-Blue (iNtRON Biotechnology, Seongnam, South Korea) was added to each fraction to extract RNA. 8-(4-Chlorophenylthio) adenosine 3',5'-cyclic monophosphate sodium salt (pCPT-cAMP; C-3912) and RU486 (M-8046) were purchased from Merck.

### **Plasmids, si-RNAs, ASO, and Adenovirus Infusion**

The eukaryotic expression vector encoding GR was described previously (Xie et al., 2009). and that encoding mouse hnRNPL was constructed by cloning cDNA (MR208796, OriGene, Rockville, MD) into p3XFLAG-CMV-10 (Sigma-Aldrich) through conventional gene recombination. To construct eukaryotic expression vector for *Ctcflos*, the *Ctcflos* 202-S2 fragments amplified from the mouse liver cDNA was cloned into pCDNA 3.1 plus. si-RNAs targeting mouse GR, hnRNPL, and GFP were synthesized by Bioneer Co. (Daejeon, South Korea) (Supplementary Table). The antisense oligonucleotide (ASO) targeting *Ctcflos*, ASO-*Ctcflos*, was synthesized by Qiagen (Hilden, Germany) (Supplementary Table). Transient transfection of si-RNAs and ASO was performed using Lipofectamine 2000 (Invitrogen, Carlsbad, CA), as described previously (Han et al., 2019). The adenovirus encoding *Ctcflos*, Ad-*Ctcflos*, was constructed by recombination of pcDNA3.1 encoding *Ctcflos* with an adenoviral backbone plasmid, pAdEasy-1. The titers of the adenovirus preparations were determined by plaque counts. Ad-*Ctcflos* was generated and kindly provided by Dr. SH. Koo (Division of Life Sciences, Korea University, Seoul, Korea). Transduction of the adenovirus was conducted as described previously (Kim et al., 2012).

### **Animal Experiments**

Eight-week-old male C57BL/6N mice were obtained from Orient Bio Inc. (Seongnam, South Korea) and housed in an air-conditioned room at 22–24°C and 50%–60% humidity with a 12-h light/dark cycle. To analyze the tissue distribution of *Ctcflos*, *Pck1*, and *Ctcf1* in mice, eight tissues, including the liver and kidney, were dissected from mice and rapidly excised, and portions of tissues were stored for further experiments. To establish the fasting or feeding conditions, mice were fasted for 24 h or fed *ad libitum*. Dexamethasone dissolved in 5% DMSO and 45% PEG30 was administered at a dose of 1 mg/kg of body weight 1 h prior to sacrifice. To overexpress *Ctcflos* in the liver, Ad-*Ctcflos* or Ad-GFP ( $1.0 \times 10^9$  plaque-forming units/mouse) was injected into mice via the tail vein. On the 7<sup>th</sup> day, the mice were fasted for 24 h and liver tissues were collected. All animal experiments were conducted according to the guidelines of the Seoul National University Institutional Animal Care and Use Committee (SNU-200407-3).

### **Analysis of Chromatin Immunoprecipitation Sequencing (ChIP-seq) Data and ChIP Analysis**

The binding signals of H3K27ac, H3K4me3, H3K4me1, and GR on the mouse *Pck1* enhancer region were identified in the Gene Expression Omnibus database (GSE31039, GSE72087, and GSE46047). To visualize ChIP-seq from the public database, we used the Integrative Genomics Viewer Software (Broad Institute, Cambridge, MA). The ChIP assay was conducted using the following antibodies: anti-H3K27ac (ab4729, Abcam, Cambridge, UK), anti-H3K4me3 (ab8580, Abcam), anti-H3K4me1 (ab8895, Abcam), anti-

GR (24050-1-AP, Proteintech, Rosemont, IL), or anti-hnRNPL (ab6106, Abcam); or control IgG (SC-2025, Santa Cruz Biotechnology, Santa Cruz, CA, and 2729s, Cell Signaling Technology, Danvers, MA), as described previously (Kim et al., 2017). The immunoprecipitated genome region was amplified using the SYBR Green Master mix (Applied Biosystems, Foster City, CA) with specific primers (Supplementary Table). Data were normalized to the input and analyzed relative to the nonspecific IgG control.

### **Rapid Amplification of cDNA Ends (RACE)**

Total RNA was isolated from the primary mouse hepatocytes using an RNeasy Mini kit according to the manufacturer's protocol (Qiagen). The GeneRacer™ Kit (Invitrogen) was used to amplify the 5' and 3' RACE-ready cDNAs according to the manufacturer's instructions. Briefly, 2.5 mg of total RNA was subjected to GeneRacer Oligo ligation and then the M-MLV reverse transcriptase (Invitrogen) was used to produce RACE-ready cDNAs. The RACE and nested RACE PCRs were performed using Biotechnology i-StarTaq™ DNA Polymerase (iNtRON Biotechnology). RACE-specific primers were designed by Integrated DNA technologies. The resulting RACE PCR products were cloned using the TOPO TA cloning kit (Invitrogen) and sequenced.

### **PCR and Quantitative Real-time PCR (qPCR)**

Total RNA was extracted from primary hepatocytes using easy-BLUE™ (iNtRON Biotechnology) according to the manufacturer's instructions. Total RNA was reverse transcribed with M-MLV reverse transcriptase (Invitrogen) and PCR was performed using specific primers (Supplementary Table). PCR products were analyzed by ethidium-bromide-containing agarose gel electrophoresis. qPCR was performed using an ABI StepOnePlus™ Real-time PCR system (Applied Biosystems). Relative RNA levels were measured using the equation  $2^{-\Delta\Delta Ct}$  ( $\Delta\Delta Ct = Ct$  of the target gene –  $Ct$  of 18S rRNA) and are presented as fold change from the level of the control, which was designated as 1 (Han et al., 2014).

### **Western Blotting, Co-immunoprecipitation, and *in situ* Proximity Ligation Assays (PLAs)**

Western blotting was basically performed as described previously using specific antibodies against Pck1 (ab28455, Abcam), hnRNPL (ab6106, Abcam), GR (12041s, Cell Signaling), or b-actin (SC-47778, Santa Cruz), or control IgG (SC-2025, Santa Cruz or 2729s, Cell Signaling) (Kim *et al.*, 2017). The coimmunoprecipitation assay was performed using specific antibodies against GR (24050-1-AP, Proteintech) and hnRNPL (ab6106, Abcam), as described previously (Ka et al., 2017). *In situ* PLAs were performed using the Duolink In Situ Red Starter Kit Mouse/Rabbit (Sigma-Aldrich), as described previously (Ka *et al.*, 2017). Briefly, cells grown in 8-well chamber slides were transfected with 20 pmol ASO-*Ctcflos*. Cells were fixed and incubated with primary antibodies against GR (24050-1-AP, Proteintech) and hnRNPL (ab6106, Abcam). The slides were incubated with PLA probes and subsequent ligation and rolling-circle amplification were performed. The PLA signals were visualized using a Zeiss LSM 710 confocal microscope.

## Reporter Gene Analysis

The enhancer region of *Pck1* (chr 2: 172,965,854–172,966,544) was amplified from the mouse genomic DNA (G3091, Promega, Madison, WI, USA) as a template using the Pfu-X polymerase (SolGent, Daejeon, South Korea). The obtained DNA fragment was cloned into the *MluI/BglII* site upstream of the luciferase coding region of the pGL2-promoter vector (Promega) by conventional gene recombination. For reporter gene assays, AML12 cells were transfected with the *Pck1* enhancer-Luc reporter and eukaryotic expression vectors encoding GR and hnRNPL using Lipofectamine<sup>TM</sup> 2000 (Invitrogen). Luciferase activity was normalized to b-galactosidase activity, as described previously (Han *et al.*, 2019).

## RNA Pull-down Assay

*Ctcflos* and its antisense strand were synthesized *in vitro* using the MEGAscript T7/SP6 Transcription Kit (Invitrogen) and biotinylated using a Biotin RNA Labeling mix (Roche). After purification, RNAs were diluted using an RNA structure buffer (10 mM Tris-Cl pH 7.0, 0.1 M KCL, and 10 mM MgCl<sub>2</sub>) to induce proper RNA folding. Nuclear pellets were obtained from primary hepatocytes and resuspended in RNA immunoprecipitation buffer (150 mM KCl, 25 mM Tris pH 7.4, 5 mM EDTA, 0.5% NP-40, 0.5 mM DTT, 100 U/mL RNase inhibitor, and protease inhibitor cocktail). The suspended nuclei were sheared using a Dounce homogenizer. Aliquots of 30 pmol of folded RNAs were added to the pre-cleared nuclear lysates and incubated at 4°C for 2 h with agitation. Streptavidin-conjugated agarose beads (Millipore, Billerica, MA) were added and incubated at 4°C for 1 h with agitation. The beads were washed with the RNA immunoprecipitation buffer and boiled in SDS sample buffer. The resulting protein mixture was applied to gel electrophoresis and visualized by silver staining. The target protein band was analyzed by mass spectrometry.

## Statistics

GraphPad Prism (<https://www.graphpad.com/>) (GraphPad Software) was applied to all data obtained in this research. All values are expressed as the mean ± standard deviation (SD) based on three independent experiments, unless indicated otherwise. Statistical analysis was performed using the nonparametric Mann–Whitney *U* test or unpaired Student's *t*-test for simple comparison. *P* < 0.05 was considered statistically different.

# Results

## Identification of *Ctcflos* Transcripts in the Enhancer Region of the Mouse *Pck1* Gene

To understand better the molecular mechanisms underlying the transcriptional expression of *Pck1*, we analyzed the ChIP-seq database obtained from the NCBI Gene Expression Omnibus database (GSE31039). In the 28 Kb upstream region of the mouse *Pck1* gene, we found a potential enhancer site marked with H3K4me1 and H3K27ac (mouse chromosome 2: 172,965,854–172,966,544) (Fig. 1A). The *Pck1* enhancer region overlapped with the first exon and upstream region of the lncRNA annotated as

*Ctcflos*-204 (Fig. 1A and 1B). *Ctcflos* (from “CCCTC-binding factor (zinc finger protein)-like, opposite strand”; NCBI Reference Sequence NR\_040321.1; gene name ENSMUSG00000087382, aka 1300015D01Rik) was annotated as four different transcripts, *Ctcflos*-201, -202, -203, and -204, located at 172,952,611-172,974,997 of the mouse chromosome 2, according to the Ensembl and NCBI gene database. First, we characterized the *Ctcflos* transcripts in the mouse liver by performing RACE. We identified five different transcripts, one of which, *Ctcflos*-202, was the same as the transcript annotated in the Ensembl database. The others had additional sequences in the intron between exons 3 and 4 of 202, and were termed *Ctcflos*-202-S1, -202-S2, -202-L1, and -202-L2. Moreover, *Ctcflos*-202-L1 and *Ctcflos*-202-L2 contained extra sequences at the 3' end, as shown in Fig. 1B. Next, we measured the level of *Ctcflos* transcripts in different mouse tissues using primers that detect all forms of *Ctcflos* (Supplementary Table). The levels of the *Ctcflos* and *Pck1* transcripts were higher in the liver, whereas transcripts of *Ctcf1*, a 5' neighboring gene of *Ctcflos*, were abundant only in the testes (Fig. 1C). *Ctcflos* was distributed mostly in the chromatin and nucleoplasm fractions of mouse hepatocytes, which may indicate potential roles for this lncRNA in the nucleus, probably in the control of gene expression (Fig. 1D).

### Expression of *Ctcflos* is GR Dependent

To identify potential functions of *Ctcflos* in the control of the expression of the *Pck1* gene, we examined the level of the transcripts in fed and fasted mice. Interestingly, the mRNA levels of both *Ctcflos* and *Pck1* were increased in the liver of fasted mice. The analysis of the expression of each *Ctcflos* isotype using specific primers revealed that the levels of all isotypes were increased in the fasted liver (Fig. 2A). However, the levels of *Ctcflos*-202-S1 and *Ctcflos*-202-S2 were not determined accurately because of the lack of specific primers for these transcripts. Similar results were obtained when mice were administered dexamethasone and cAMP, which are well-known inducers of *Pck1* gene expression (Fig. 2B). These results indicated that *Ctcflos* might have a function in the transcription of the *Pck1* gene. Moreover, these findings suggested that GR was associated with the induction of *Ctcflos*.

To examine the involvement of GR in the expression of *Ctcflos*, publicly available ChIP-seq data (GSE72087 and GSE46047) were analyzed (Goldstein et al., 2017; Grontved et al., 2013). Surprisingly, GR binding was enriched in the *Pck1* enhancer as well as in the promoter region in the liver of fasted and dexamethasone-administered mice (Fig. 3A) (Hanson and Reshef, 1997). Consistently, the ChIP analysis demonstrated that DNA binding of GR in the *Pck1* enhancer and the promoter sites was increased in the liver of these mice (Fig. 3B). In addition, the DNA binding signals of H3K4me1 and H3K27ac were enriched in the *Pck1* enhancer region, whereas those of H3K4me3 and H3K27ac were enriched in the promoter region (Fig. 3B). These results indicated that GR binding in the enhancer region may induce transcriptional activation of the *Pck1* gene. Furthermore, knockdown of GR expression by si-RNA decreased largely the level of *Ctcflos* in the primary hepatocytes (Supplementary Fig. 1A). It also decreased the level of *Pck1* protein levels (Fig. 3C, Supplementary Fig. 2). Moreover, suppression of GR activity using a GR antagonist, RU486, inhibited the dexamethasone/cAMP-induced *Ctcflos* and *Pck1* expression in the primary hepatocytes (Fig. 3D). Lastly, we delineated six potential GREs in the *Pck1* enhancer region by in silico analysis (Fig. 3E). The luciferase reporter encoding the *pck1* enhancer was



activated by transient expression of GR (Fig. 3E). Taken together, these results suggested that the expression of *Ctcflos* was GR dependent.

### **Ctcflos Enhances the Transcription of the Mouse Pck1 Gene**

To examine whether *Ctcflos* plays a role in the transcriptional expression of *Pck1*, we generated an adenovirus encoding *Ctcflos*, Ad-*Ctcflos*. Infusion of Ad-*Ctcflos* in the primary hepatocytes increased the level of *Pck1* transcripts in the presence of dexamethasone (Fig. 4A). Tail-vein injection of Ad-*Ctcflos* increased the level of the Pck1 protein in the mouse liver (Fig. 4B). Knockdown of *Ctcflos* by transfection of the antisense oligonucleotide (ASO)-*Ctcflos* decreased largely the level of *Pck1* transcripts in the primary hepatocytes. However, ASO-*Ctcflos* did not significantly change the transcript levels of the *Ctcflos* or representative GR-responsive genes, such as *G6pc* (encoding glucose-6-phosphatase, catalytic subunit) and *Tat* (encoding tyrosine aminotransferase) (Fig. 4C) (Grange et al., 2001; Vander Kooi et al., 2005). Consistently, transfection of ASO-*Ctcflos* decreased the levels of the Pck1 protein (Fig. 4D). Taken together, these results demonstrated that *Ctcflos* enhanced the transcription of the mouse *Pck1* gene.

### **Interaction between Ctcflos and hnRNPL Enhances the GR-mediated Pck1 Gene Expression**

To understand the mechanism via which *Ctcflos* enhances GR-mediated *Pck1* gene expression, we performed RNA pull-down assays to search for *Ctcflos*-binding proteins. As shown in Fig. 5A, a specific protein band was pulled down by *in vitro* transcribed biotinylated-Sense-*Ctcflos*. The LC-MS/MS analysis of this protein band revealed that hnRNPL interacted with *Ctcflos*. The binding of *Ctcflos* and hnRNPL was further confirmed by western blotting of the pulled down protein mixture using a specific antibody to hnRNPL (Fig. 5B). Next, we examined whether hnRNPL bound to GR, as the function of *Ctcflos* was GR dependent. Surprisingly, we found that hnRNPL was physically associated with GR in co-immunoprecipitation assays (Fig. 5C). Furthermore, the CHIP analysis showed that GR bound to the *Pck1* enhancer region in the presence of dexamethasone/cAMP, the condition in which the amount of *Ctcflos* increased in the primary hepatocytes. However, hnRNPL did not bind to the *Pck1* enhancer in the presence or absence of dexamethasone, which suggests that *Ctcflos* affects the interaction between hnRNPL and GR (Fig. 5D). In fact, the binding of hnRNPL and GR increased after transfection of ASO-*Ctcflos* in co-immunoprecipitation assays (Fig. 5E). The dissociation of GR and hnRNPL in the presence of ASO-*Ctcflos* was confirmed by *in situ* PLA assays in that the number of fluorescent puncta formed by the interaction of GR with hnRNPL increased in the presence of ASO-*Ctcflos* (Fig. 5F). Furthermore, GR binding in the *Pck1* enhancer region was decreased in the presence of ASO-*Ctcflos*. Similarly, GR binding in the *Pck1* promoter was decreased, indicating that the GR-mediated *Pck1* gene activation was suppressed in the presence of ASO-*Ctcflos* (Fig. 5G). Taken together, these results indicate that *Ctcflos* interferes with the binding of GR to hnRNPL, which subsequently increases GR recruitment in the *Pck1* enhancer region, resulting in transcriptional activation of the *Pck1* gene in the presence of dexamethasone.

As expected, silencing of hnRNPL using si-RNA increased the level of *Ctcflos* in the primary hepatocytes (Fig. 6A, Supplementary Fig. 1B). Moreover, it increased the transcript and protein levels of Pck1 in the

presence of dexamethasone/cAMP (Fig. 6A and 6B). Consistently, transient transfection of hnRNPL suppressed the GR-induced *Pck1* enhancer activity, whereas overexpression of *Ctcflos* recovered the hnRNPL-mediated suppression of the *Pck1* enhancer activity (Fig. 6C).

## Discussion

*Pck1* is a key enzyme that catalyzes an irreversible step of hepatic gluconeogenesis; however, the mechanisms underlying *Pck1* gene expression have not been fully identified. Here, we report that *Ctcflos*, a liver-enriched lncRNA encoded in the *Pck1* enhancer region, regulated hepatic expression of the *Pck1* gene under fasting conditions. Moreover, it enhanced the expression of *Pck1* at the transcription level in a GR-dependent manner through binding to hnRNPL, which represents a novel regulatory mechanism of *Pck1* gene transcription (Fig. 6D).

Recently, a diverse molecular mechanism was described to explain how nuclear lncRNAs regulate the expression of target genes. We showed that *Ctcflos* regulates the expression of the *Pck1* gene by directly interacting with hnRNPL, a key RNA regulatory factor (Geuens et al., 2016). hnRNPL plays roles in the alternative splicing of RNA and maintenance of mRNA stability, probably through binding to CA-repeat motifs within the 3'-UTR of mRNA (Hui et al., 2005; Hui et al., 2003). Interestingly, we found similar CA-rich motifs in the second exon of the *Ctcflos*-202-S2 and *Ctcflos*-202-L2 forms, although it was not clear whether the motifs were involved in the binding of *Ctcflos* to hnRNPL. Moreover, other studies showed that several lncRNAs interact with hnRNPL. For example, lncRNA *THRIL* enhanced the expression of TNF $\alpha$  through its interaction with hnRNPL in the TNF $\alpha$  promoter region (Li et al., 2014). Furthermore, *lncLGR* facilitates the recruitment of hnRNPL to the mouse glucokinase promoter, to suppress the transcription of the gene in the liver (Ruan et al., 2016), and *linc-AAM* interacts with hnRNPL, thereby repressing the expression of immune response genes such as *IL-6*, *COX-2*, and *TNF- $\alpha$*  in macrophages in mice (Chen et al., 2021). These findings suggest that hnRNPL functions as an adaptor that links lncRNA to a specific effector to control target gene expression. We suggest that GR is the specific effector of *Ctcflos*, as the binding of hnRNPL to GR was abolished in the presence of *Ctcflos* (Fig. 5D). Further studies of hnRNPL, including global screening of interacting proteins and lncRNAs, are guaranteed to promote the understanding of the complicated network of intracellular macromolecules governing diverse physiological phenomena at the molecular level.

Because the genetic location of *Ctcflos* overlaps with that of the *Ctcf1* gene, a *cis*-regulatory role of *Ctcflos* in *Ctcf1* gene expression was expected (Fig. 1A, 1B). *Ctcf1* (also known as brother of regulator of imprinted sites) is a transcription factor that forms a methylation-sensitive insulator resulting in X-chromosome inactivation. It was previously reported that *Ctcf1* is abundantly expressed in the cytoplasm of testicular germ cells (Loukinov et al., 2002). Consistently, we found that *Ctcf1* transcripts were mostly present in the mouse testes, which is different from that observed for *Ctcflos* transcripts, which were mostly present in the liver (Fig. 1C). Moreover, knockdown of *Ctcflos* did not affect the expression level of the *Ctcf1* mRNA, indicating that *Ctcflos* is not a regulator of *Ctcf1* gene expression (Fig. 4C). Furthermore, *Ctcflos* did not affect the expression of other GR downstream genes, such as *G6pc* and *Tat* (Fig. 4C) (Grange et al.,

2001). Taken together, our results suggest that the *cis*-acting mechanism of *Ctcflos* is specific to the hepatic transcription of the *Pck1* gene in mice.

The human homologous lncRNA of *Ctcflos* might be predicted as the putative lncRNA located on chromosome 20: 57,550,058–57,558,997 between the *Ctcf1* and *Pck1* genes (NONCODE: NONHSAT080509.2). Although there is no significant homology in their nucleotide sequences in this region in the mouse and human cases, the proximity of the putative human *Ctcflos* homolog to the *Pck1* gene suggests a possible *cis*-regulatory role for the lncRNA in the *Pck1* gene in humans. The identification and characterization of the human *Ctcflos* homolog remain to be accomplished, to further our understanding of hepatic gluconeogenesis and related metabolic diseases in humans.

The ASOs are short synthetic single-stranded nucleotides complementary to the RNA target that suppress the expression of genes with multiple mechanisms, including RNA degradation via RNase H endonuclease, alteration of the splicing process, and changing the steric hindrance of ribosomal activity for the translation of target RNAs (Crooke, 2017; Roberts et al., 2020). As coding and non-coding RNAs represent a unique target for developing therapeutics, ASO compounds have been subjected to diverse modification of their chemical structures to enhance their potential as effective therapeutics with increased lipid solubility and decreased off-target effects (Crooke et al., 2020). Because of these successful strategies, recently, several ASO therapeutics have been developed and many are currently in clinical stages of investigation (Winkle et al., 2021). Previously, an ASO targeting GR was examined for its impact on the diabetic syndrome in *ob/ob* and *db/db* mice. The ASO inhibited GR expression and improved blood glucose control under diabetic conditions, suggesting the potential of the ASO for the control of gluconeogenesis (Liang et al., 2005). ASO therapeutics targeting *Ctcflos* that suppress specifically the GR-mediated *Pck1* gene expression in the liver could be a better alternative to hyperglycemia treatment by avoiding systemic and global suppression of the GR-mediated physiology.

## Conclusion

*Ctcflos* is a novel lncRNA which locates in the enhancer region of mouse *Pck1* gene. It binds hnRNPL leading to dissociation of glucocorticoid receptor from the hnRNPL-glucocorticoid receptor complex, resulting in upregulation of the *Pck1* gene transcription. *Ctcflos* may provide a promising target for alternative treatment of hyperglycemia through the specific regulation of *Pck1* gene.

## Abbreviations

*Pck1*: Phosphoenolpyruvate carboxykinase; lncRNA: long non-coding RNA; GR: glucocorticoid receptor; hnRNPL: heterogeneous ribonucleoprotein L ; ASO: antisense oligonucleotide

## Declarations

*No conflicts of interest were declared.*

**Authors' Contributions.** J.Y., J.K., and M.L. designed the study and interpreted the results; J.Y., J.K., N.K., and S.L. conducted most of the in vitro and in vivo experiments; J.Y., J.K., and M.L. wrote the manuscript; M.L. supervised the research.

**Funding.** This study was supported by the National Research Foundation of Korea [2017R1A2B3011870 and 2018R1A5A2024425]; and Korea Mouse Phenotyping Project [NRF-2014M3A9D5A01073556].

**Ethics approval and consent to participate.** All animal experiments were conducted according to the guidelines of the Seoul National University Institutional Animal Care and Use Committee (SNU-200407-3).

**Consent for publication.** Not applicable

**Competing interests.** No potential conflicts of interest relevant to this article were reported.

**Availability of data and materials.** All data generated or analysed during this study are included in this published article

**Acknowledgements.** Not applicable

## References

1. Chakravarty K, Cassuto H, Reshef L, et al. Factors that control the tissue-specific transcription of the gene for phosphoenolpyruvate carboxykinase-C. *Crit Rev Biochem Mol Biol.* 2005;40(3):129-54.
2. Chen X, He Y, Zhu Y, Du J, et al. linc-AAM Facilitates Gene Expression Contributing to Macrophage Activation and Adaptive Immune Responses. *Cell Rep.* 2021;34(1):108584.
3. Crooke ST. Molecular Mechanisms of Antisense Oligonucleotides. *Nucleic Acid Ther.* 2017;27(2):70-7.
4. Crooke ST, Seth PP, Vickers TA, et al. The Interaction of Phosphorothioate-Containing RNA Targeted Drugs with Proteins Is a Critical Determinant of the Therapeutic Effects of These Agents. *J Am Chem Soc.* 2020;142(35):14754-71.
5. Gates LA, Foulds CE, O'Malley BW. Histone Marks in the 'Driver's Seat': Functional Roles in Steering the Transcription Cycle. *Trends Biochem Sci.* 2017;42(12):977-89.
6. Geuens T, Bouhy D, Timmerman V. The hnRNP family: insights into their role in health and disease. *Hum Genet.* 2016;135(8):851-67.
7. Goldstein I, Baek S, Presman DM, et al. Transcription factor assisted loading and enhancer dynamics dictate the hepatic fasting response. *Genome Res.* 2017;27(3):427-39.
8. Grange T, Cappabianca L, Flavin M, et al. In vivo analysis of the model tyrosine aminotransferase gene reveals multiple sequential steps in glucocorticoid receptor action. *Oncogene.* 2001;20(24):3028-38.
9. Grontved L, John S, Baek S, et al. C/EBP maintains chromatin accessibility in liver and facilitates glucocorticoid receptor recruitment to steroid response elements. *EMBO J.* 2013;32(11):1568-83.

10. Han YH, Kim HJ, Kim EJ, et al. RORalpha decreases oxidative stress through the induction of SOD2 and GPx1 expression and thereby protects against nonalcoholic steatohepatitis in mice. *Antioxid Redox Signal*. 2014;21(15):2083-94.
11. Han YH, Shin KO, Kim JY, et al. A maresin 1/RORalpha/12-lipoxygenase autoregulatory circuit prevents inflammation and progression of nonalcoholic steatohepatitis. *J Clin Invest*. 2019;129(4):1684-98.
12. Hanson RW, Reshef L. Regulation of phosphoenolpyruvate carboxykinase (GTP) gene expression. *Annu Rev Biochem*. 1997;66:581-611.
13. Hui J, Hung LH, Heiner M, et al. Intronic CA-repeat and CA-rich elements: a new class of regulators of mammalian alternative splicing. *EMBO J*. 2005;24(11):1988-98.
14. Hui J, Reither G, Bindereif A. Novel functional role of CA repeats and hnRNP L in RNA stability. *RNA*. 2003;9(8):931-6.
15. Imai E, Stromstedt PE, Quinn PG, et al. Characterization of a complex glucocorticoid response unit in the phosphoenolpyruvate carboxykinase gene. *Mol Cell Biol*. 1990;10(9):4712-9.
16. Jitrapakdee S. Transcription factors and coactivators controlling nutrient and hormonal regulation of hepatic gluconeogenesis. *Int J Biochem Cell Biol*. 2012;44(1):33-45.
17. Ka NL, Na TY, Na H, et al. NR1D1 Recruitment to Sites of DNA Damage Inhibits Repair and Is Associated with Chemosensitivity of Breast Cancer. *Cancer Res*. 2017;77(9):2453-63.
18. Kim EJ, Yoon YS, Hong S, et al. Retinoic acid receptor-related orphan receptor alpha-induced activation of adenosine monophosphate-activated protein kinase results in attenuation of hepatic steatosis. *Hepatology*. 2012;55(5):1379-88.
19. Kim HJ, Han YH, Na H, et al. Liver-specific deletion of RORalpha aggravates diet-induced nonalcoholic steatohepatitis by inducing mitochondrial dysfunction. *Sci Rep*. 2017;7(1):16041.
20. Kopp F, Mendell JT. Functional Classification and Experimental Dissection of Long Noncoding RNAs. *Cell*. 2018;172(3):393-407.
21. Li T, Huang X, Yue Z, et al. Knockdown of long non-coding RNA Gm10804 suppresses disorders of hepatic glucose and lipid metabolism in diabetes with non-alcoholic fatty liver disease. *Cell Biochem Funct*. 2020;38(7):839-46.
22. Li W, Notani D, Rosenfeld MG. Enhancers as non-coding RNA transcription units: recent insights and future perspectives. *Nat Rev Genet*. 2016;17(4):207-23.
23. Li Z, Chao TC, Chang KY, et al. The long noncoding RNA THRIL regulates TNFalpha expression through its interaction with hnRNPL. *Proc Natl Acad Sci U S A*. 2014;111(3):1002-7.
24. Liang Y, Osborne MC, Monia BP, et al. Antisense oligonucleotides targeted against glucocorticoid receptor reduce hepatic glucose production and ameliorate hyperglycemia in diabetic mice. *Metabolism*. 2005;54(7):848-55.
25. Local A, Huang H, Albuquerque CP, et al. Identification of H3K4me1-associated proteins at mammalian enhancers. *Nat Genet*. 2018;50(1):73-82.

26. Loukinov DI, Pugacheva E, Vatolin S, et al. BORIS, a novel male germ-line-specific protein associated with epigenetic reprogramming events, shares the same 11-zinc-finger domain with CTCF, the insulator protein involved in reading imprinting marks in the soma. *Proc Natl Acad Sci U S A*. 2002;99(10):6806-11.
27. Miao Y, Ajami NE, Huang TS, et al. Enhancer-associated long non-coding RNA LEENE regulates endothelial nitric oxide synthase and endothelial function. *Nat Commun*. 2018;9(1):292.
28. Mostafa MM, Bansal A, Michi AN, et al. Genomic determinants implicated in the glucocorticoid-mediated induction of KLF9 in pulmonary epithelial cells. *J Biol Chem*. 2021;296:100065.
29. Puigserver P, Rhee J, Donovan J, et al. Insulin-regulated hepatic gluconeogenesis through FOXO1-PGC-1alpha interaction. *Nature*. 2003;423(6939):550-5.
30. Roberts TC, Langer R, Wood MJA. Advances in oligonucleotide drug delivery. *Nat Rev Drug Discov*. 2020;19(10):673-94.
31. Roqueta-Rivera M, Esquejo RM, Phelan PE, et al. SETDB2 Links Glucocorticoid to Lipid Metabolism through Insig2a Regulation. *Cell Metab*. 2016;24(3):474-84.
32. Ruan X, Li P, Cangelosi A, et al. A Long Non-coding RNA, IncLGR, Regulates Hepatic Glucokinase Expression and Glycogen Storage during Fasting. *Cell Rep*. 2016;14(8):1867-75.
33. Rui L. Energy metabolism in the liver. *Compr Physiol*. 2014;4(1):177-97.
34. Saltiel AR, Kahn CR. Insulin signalling and the regulation of glucose and lipid metabolism. *Nature*. 2001;414(6865):799-806.
35. Sartorelli V, Lauberth SM. Enhancer RNAs are an important regulatory layer of the epigenome. *Nat Struct Mol Biol*. 2020;27(6):521-8.
36. Sasse SK, Gruca M, Allen MA, et al. Nascent transcript analysis of glucocorticoid crosstalk with TNF defines primary and cooperative inflammatory repression. *Genome Res*. 2019;29(11):1753-65.
37. Statello L, Guo CJ, Chen LL, et al. Gene regulation by long non-coding RNAs and its biological functions. *Nat Rev Mol Cell Biol*. 2021;22(2):96-118.
38. Vander Kooi BT, Onuma H, Oeser JK, et al. The glucose-6-phosphatase catalytic subunit gene promoter contains both positive and negative glucocorticoid response elements. *Mol Endocrinol*. 2005;19(12):3001-22.
39. Volpe CMO, Villar-Delfino PH, Dos Anjos PMF, et al. Cellular death, reactive oxygen species (ROS) and diabetic complications. *Cell Death Dis*. 2018;9(2):119.
40. Wang J, Yang W, Chen Z, et al. Long Noncoding RNA IncSHGL Recruits hnRNPA1 to Suppress Hepatic Gluconeogenesis and Lipogenesis. *Diabetes*. 2018;67(4):581-93.
41. Weikum ER, Knuesel MT, Ortlund EA, et al. Glucocorticoid receptor control of transcription: precision and plasticity via allostery. *Nat Rev Mol Cell Biol*. 2017;18(3):159-74.
42. Winkle M, El-Daly SM, Fabbri M, et al. Noncoding RNA therapeutics - challenges and potential solutions. *Nat Rev Drug Discov*. 2021;20(8):629-51.

43. Xie YB, Nedumaran B, Choi HS. Molecular characterization of SMILE as a novel corepressor of nuclear receptors. *Nucleic Acids Res.* 2009;37(12):4100-15.
44. Yang J, Reshef L, Cassuto H, et al. Aspects of the control of phosphoenolpyruvate carboxykinase gene transcription. *J Biol Chem.* 2009;284(40):27031-5.
45. Yoon JC, Puigserver P, Chen G, et al. Control of hepatic gluconeogenesis through the transcriptional coactivator PGC-1. *Nature.* 2001;413(6852):131-8.
46. Zhao Y, Wu J, Liangpunsakul S, et al. Long Non-coding RNA in Liver Metabolism and Disease: Current Status. *Liver Res.* 2017;1(3):163-7.

## Figures

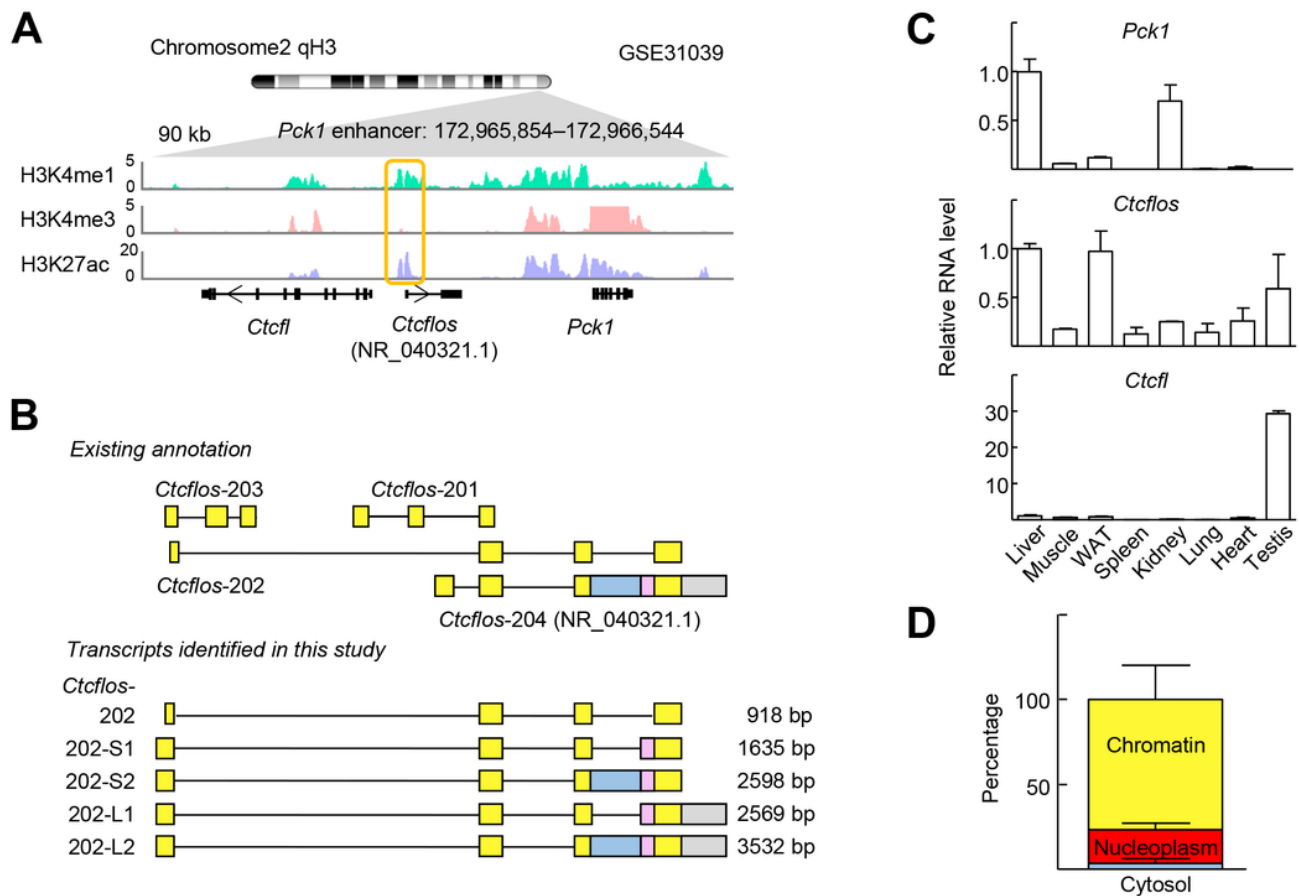


**Figure 1**

Gene structure and tissue distribution of the mouse *Ctcfls*. A: Schematic representation of a potential enhancer of *Pck1* gene in mice. Database-based ChIP-seq analysis was conducted using public datasets obtained from the NCBI GEO database (GSE31039). H3K27ac H3K4me3, and H3K4me1 in the genome

loci of *Pck1* gene are shown in ChIP-seq track. The potential *Pck1* enhancer (chr 2: 172,965,854 -172,966,544) was indicated by an orange box. B: Transcripts of *Ctcflos* (NCBI Reference Sequence NR\_040321.1; gene name ENSMUSG00000087382, aka 1300015D01Rik) are annotated previously in Ensembl and NCBI database (top). Transcripts of *Ctcflos* those were identified by RACE in this study. Total RNA was isolated from the primary mouse hepatocytes to produce RACE-ready cDNAs. RACE and nested RACE PCR were performed using specific primers and the obtained PCR products were cloned and sequenced. The size of transcript was shown in parenthesis (bottom). C: Distribution of *Ctcflos*, *Pck1* and *Ctcf1* in different organs of the C57BL/6N mice. RNA isolated from each mouse organ was subjected to the qPCR analysis using primers that amplify all isoforms of *Ctcflos*. The data represent mean  $\pm$  SD (n=3). D: The cytosol- (sky blue), nucleoplasm- (red), and chromatin-enriched (yellow) RNAs in subcellular fractions of the primary hepatocytes were purified. The RNA levels of *Ctcflos* were analyzed by qPCR. The data represent mean  $\pm$  SD (n=3).

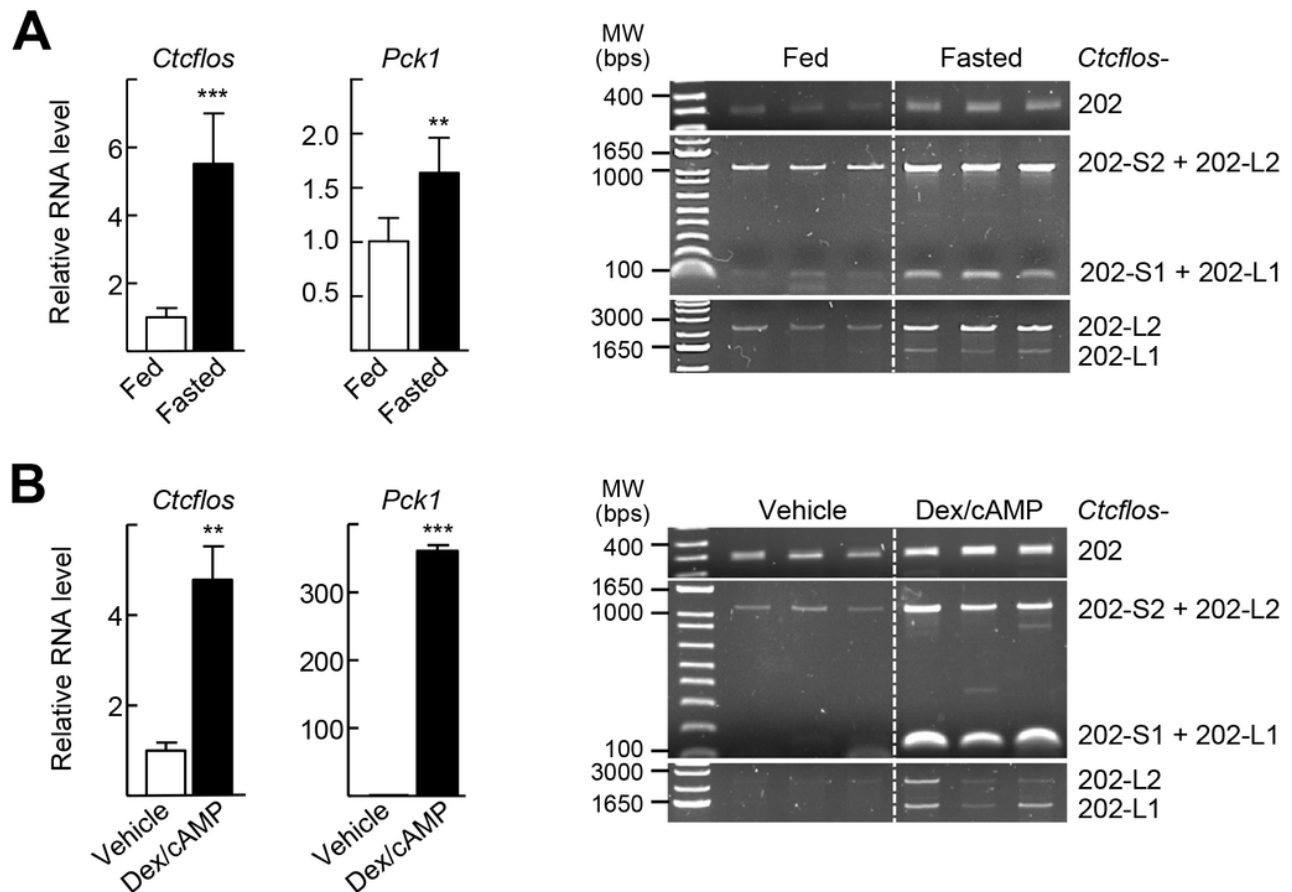


**Figure 2**

Expression of *Ctcflos* is induced in the mouse liver under fasting conditions. A: Mice were fasted or fed ad libitum for 24 h. Total RNA was obtained from the liver and RNA levels of all isoforms of *Ctcflos* and *Pck1* were analyzed by qPCR (left). Data were analyzed by Mann-Whitney U test. \*\*P < 0.01 and \*\*\*P < 0.001 vs



Feeding (n=5). The levels of different *Ctcflos* transcripts were analyzed by PCR using specific primers that distinguish each transcript. The resulting PCR products were visualized by agarose gel electrophoretogram (right). B: The primary mouse hepatocytes were treated with 100 nM dexamethasone (Dex) and 1  $\mu$ M cAMP for 6 h. The RNA levels of *Ctcflos* and *Pck1* were analyzed by qPCR (left). Data were analyzed by unpaired Student's t-test. \*\*P < 0.01 and \*\*\*P < 0.001 vs Feeding or Vehicle (n=3). The levels of different *Ctcflos* transcripts were analyzed by PCR using specific primers that distinguish each transcript. The resulting PCR products were visualized by agarose gel electrophoretogram (right).

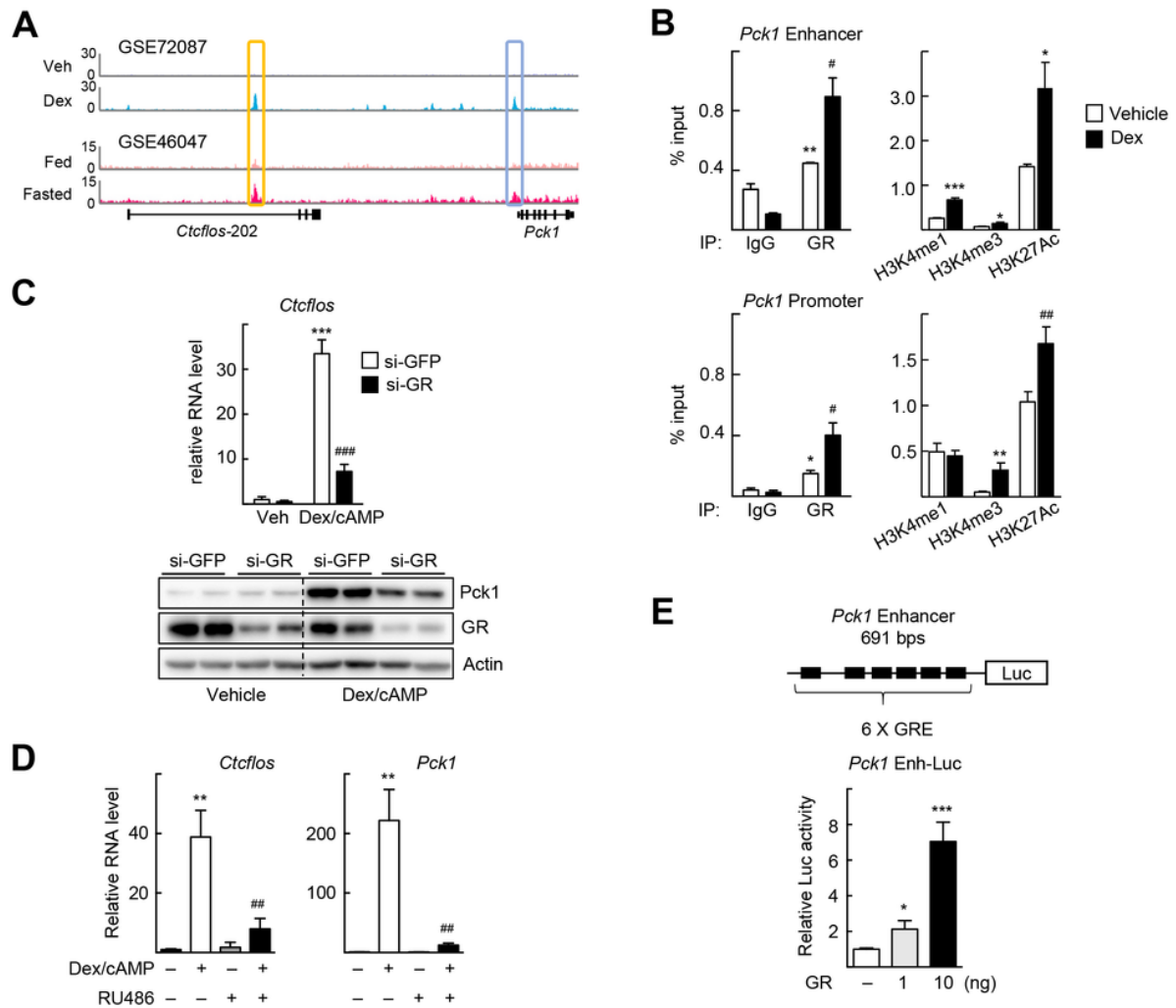


**Figure 3**

GR binds the *Pck1* enhancer region and thereby induces *Ctcflos* expression. A: ChIP-seq analysis was conducted based on GEO public datasets. GR enriched sites in the genome loci of *Pck1* gene are indicated by boxes; Orange, *Pck1* Enhancer, and Skyblue, *Pck1* Promoter. B: ChIP analysis using indicated antibodies in the enhancer and promoter regions of *Pck1* gene. Vehicle or dexamethasone (1 mg/kg BW) was administered to mice by i.p. injection at 1 h prior to sacrifice. DNA fragments were immunoprecipitated with the indicated antibodies and the enhancer region was amplified by qPCR using specific primers. Data were analyzed by unpaired Student's t-test. \*P < 0.05, \*\* P < 0.005, and \*\*\* P < 0.001 vs IgG with Vehicle; # P < 0.05 vs GR with Vehicle (n=3). C: The primary mouse hepatocytes were

transfected with si-GFP or si-GR and treated with 100 nM Dexamethasone (Dex) and 1  $\mu$ M cAMP for 6 h. The RNA levels of *Ctcflos* was analyzed by qPCR using *Ctcflos*-b primer (top). The protein levels of *Pck1* and GR were analyzed by western blotting. The band intensity was quantified and shown in Supplementary Fig. 2 (bottom). D: The primary mouse hepatocytes were treated with 100 nM Dex and 1  $\mu$ M cAMP in the presence or absence of 10  $\mu$ M RU486 for 6 h. The RNA levels of *Ctcflos* and *Pck1* were analyzed by qPCR using *Ctcflos*-b primer. Data were analyzed by unpaired Student's t-test. \*\* $P < 0.005$  vs Veh (-); ## $P < 0.01$  vs Dex/cAMP (n=3). E: Schematic presentation of the mouse *Pck1* Enh-Luc reporter containing six GREs (top). AML12 cells were transfected with the mouse *Pck1* Enh-Luc reporter and GR expression vector for 24 h. Data were analyzed by unpaired Student's t-test. \* $P < 0.05$  and \*\*\* $P < 0.05$  vs empty vector (-) (n=3) (bottom).

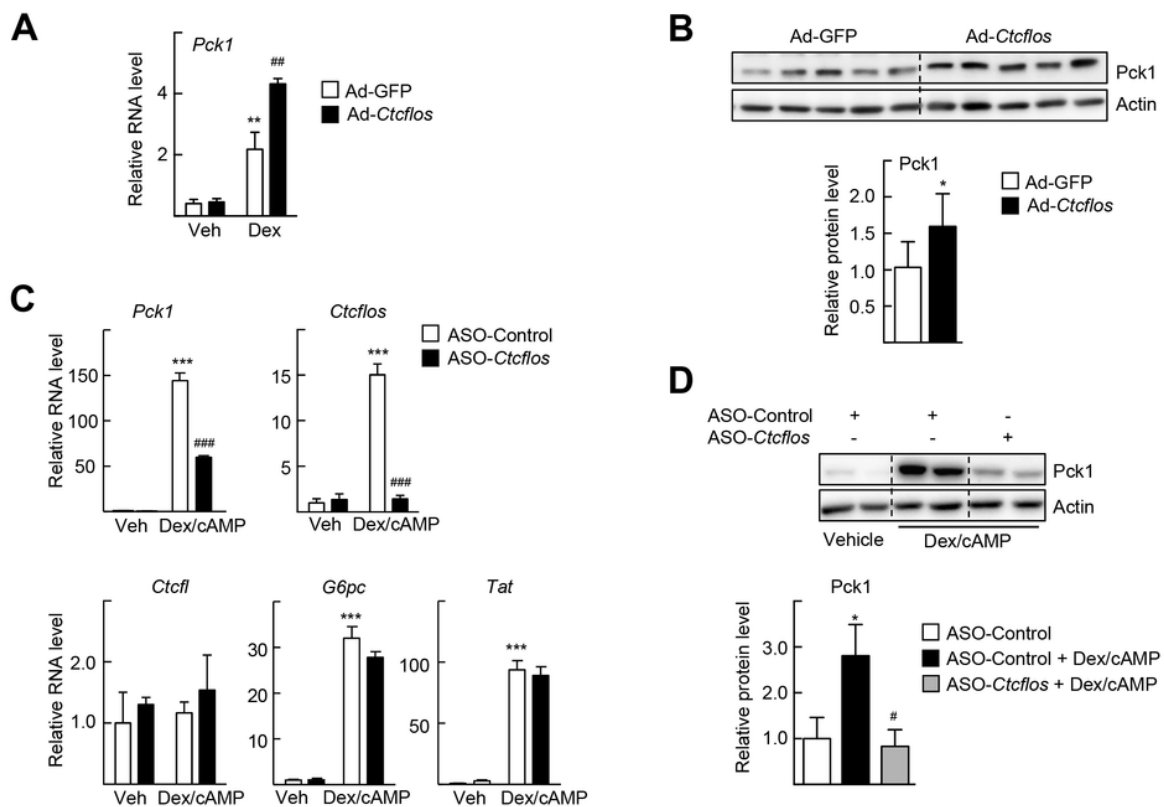


**Figure 4**

*Ctcflos* enhances transcription of *Pck1*. A: The primary mouse hepatocytes were infected by Ad-GFP or Ad-Ctcflos for 24 h and treated with vehicle (Veh) or 100 nM dexamethasone (Dex) for additional 24 h. The mRNA level of *Pck1* was analyzed by qPCR. Data were analyzed by unpaired Student's t-test. \*\* $P < 0.01$  vs Ad-GFP with Veh; ## $P < 0.01$  vs Ad-GFP with Dex (n=3). B: Ad-GFP or Ad-Ctcflos were infused into tail vein in mice. After 7 days of infusion, the liver tissues were collected for analyses. The protein level of *Pck1* was analyzed by western blotting. The intensity of band was quantified and normalized to that of

corresponding actin band. Data were analyzed by Mann-Whitney U test. \* $P < 0.05$  vs Ad-GFP ( $n=5$ ). C and D: The primary mouse hepatocytes were transfected with ASO-Control or ASO-Ctcflos and treated with 100 nM Dex and 1  $\mu$ M cAMP for 6 h. The indicated transcripts were analyzed by qRT-PCR (Ctcflos using Ctcflos-b primer) (C) and the protein level of Pck1 was analyzed by western blotting (D). The intensity of Pck1 band was quantified and normalized to that of corresponding actin band. Data were analyzed by unpaired Student's t-test. \* $P < 0.05$  and \*\*\* $P < 0.001$  vs ASO-Control with Veh; # $P < 0.05$  and ### $P < 0.001$  vs ASO-Control with Dex/cAMP ( $n=3$ ).

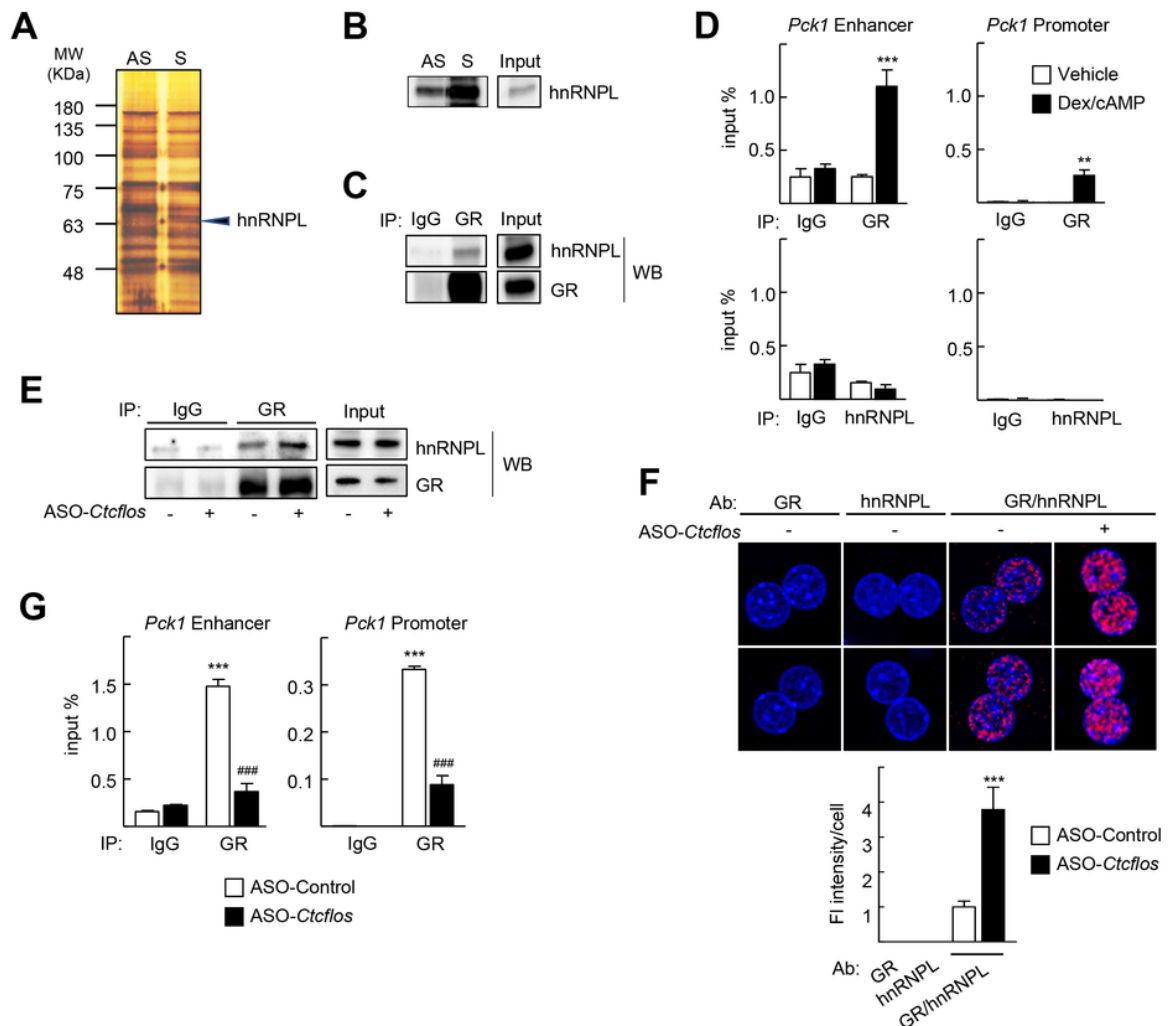


**Figure 5**

Ctcflos binds hnRNPL that interacts with GR. A and B: RNA pull-down assays were carried out using biotinylated Ctcflos (S) or its antisense (AS) with nuclear lysates prepared from the primary mouse hepatocytes. (A). The pull-downed proteins with the biotinylated Ctcflos or its antisense were analyzed by Western blotting (B). C: Whole mouse liver tissue lysates were immunoprecipitated using IgG or anti-GR antibody and probed with the indicated antibodies by western blotting. D: The primary hepatocytes were treated with Dexamethasone (Dex) and 1  $\mu$ M cAMP for 2 h. ChIP assay was conducted using indicated antibodies. The DNA fragments encoding promoter or enhancer regions of Pck1 gene were amplified using specific primers. Data were analyzed by unpaired Student's t-test. \*\* $P < 0.01$  and \*\*\* $P < 0.001$  vs

Vehicle. E-G: The primary mouse hepatocytes were transfected with ASO-Control or ASO-Ctcflos and treated with 100 nM dexamethasone (Dex) and 1  $\mu$ M cAMP for 6 h. Whole cell lysates were immunoprecipitated using IgG or anti-GR antibody and probed with the indicated antibodies by western blotting (E). PLA assay was performed to show the interaction of GR and hnRNPL (F). As negative controls, single staining with the indicated antibodies was employed. Two representative images for each condition are shown. For quantification, the fluorescence intensity per cell was measured from at least 150 cells using ImageJ software. Data were analyzed by Mann-Whitney U test. \*\*\*P < 0.001 vs ASO-Control (-) of GR/hnRNPL. ChIP assay was performed to show GR binding at the Pck1 enhancer region (G). The immunoprecipitated DNA fragments with anti-GR were amplified by qPCR using primers specific to the Pck1 enhancer and the Pck1 promoter regions. Data were analyzed by unpaired Student's t-test. \*\*\*P < 0.001 vs IgG with ASO-Control; ###P < 0.001 vs GR with ASO-Control (n=3).

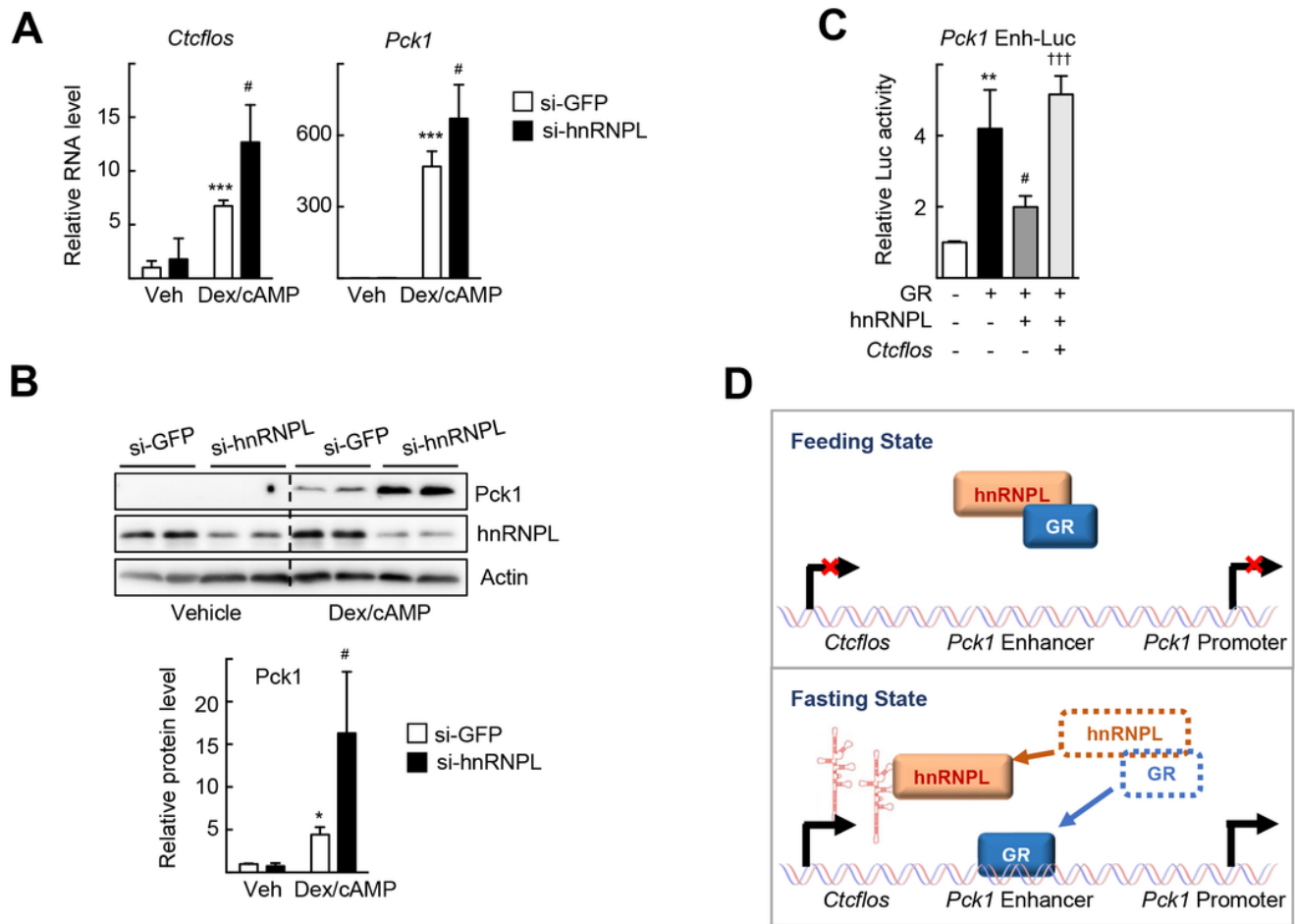


**Figure 6**

hnRNPL suppresses transcription of Pck1 gene. A and B: The primary mouse hepatocytes were transfected with si-GFP or si-hnRNPL and treated with vehicle (Veh) or 100 nM dexamethasone (Dex) and 1  $\mu$ M cAMP for 6 h. The amount of Ctcflos and the mRNA level of Pck1 were analyzed by qPCR using

using Ctcflos-b primer. Data were analyzed by unpaired Student's t-test. \*\*\* $P < 0.001$  vs si-GFP with Veh; # $P < 0.05$  vs si-GFP with Dex/cAMP (n=3) (A). The protein levels of Pck1 and hnRNPL were analyzed by western blotting. The intensity of band was quantified and normalized to that of corresponding actin band. Data were analyzed by unpaired Student's t-test. \* $P < 0.05$  vs si-GFP with Veh; # $P < 0.05$  vs si-GFP with Dex/cAMP (n=4) (B). C: AML12 cells were transfected with the Pck1 enhancer-Luc reporter and expression vector for GR, hnRNPL and/or Ctcflos. Luciferase activities were normalized by the corresponding  $\beta$ -galactosidase activity. (n=3). Data were analyzed by unpaired Student's t-test. \*\* $P < 0.01$  vs empty vector (-); # $P < 0.05$  vs GR; ††† $P < 0.001$  vs GR and hnRNPL (n=3). D: Schematic representation depicting function of Ctcflos in the transcription of Pck1 gene in the feeding and fasting transitions in the mouse liver.

## Supplementary Files

This is a list of supplementary files associated with this preprint. Click to download.

- [SupplementaryinformationMolMed.docx](#)